

Photoelectron momentum distributions of single-photon ionization under a pair of elliptically polarized attosecond laser pulses

Hui-Fang Cui(崔会芳), Xiang-Yang Miao(苗向阳)

Citation: Chin. Phys. B . 2020, 29(7): 074203 . **doi:** 10.1088/1674-1056/ab8ac0
Journal homepage: http://cpb.iphy.ac.cn; http://iopscience.iop.org/cpb

What follows is a list of articles you may be interested in

Air lasing: Phenomena and mechanisms

Helong Li(李贺龙), Danwen Yao(姚丹雯), Siqi Wang(王思琪), Yao Fu(付尧), Huailiang Xu(徐淮良)

Chin. Phys. B . 2019, 28(11): 114204 . **doi:** 10.1088/1674-1056/ab47f5

Tunneling exits of H_2^+ in strong laser fields

Zhao-Han Zhang(张兆涵), Feng He(何峰)

Chin. Phys. B . 2018, 27(10): 104203 . **doi:** 10.1088/1674-1056/27/10/104203

Multi-level effects in the high-order harmonic generation driven by intense frequency-comb laser fields

Zhao Di, Jiang Chen-Wei, Li Fu-Li

Chin. Phys. B . 2015, 24(7): 074205 . **doi:** 10.1088/1674-1056/24/7/074205

Simple formula for the ionization rate of diatomic molecules in an intense laser field using the velocity gauge

Tang Zeng-Hua, Li Yong-Qing, Ma Feng-Cai

Chin. Phys. B . 2013, 22(8): 084203 . **doi:** 10.1088/1674-1056/22/8/084203

Study of frequency-modulated excitation of Rydberg potassium atoms by using *B*-spline

Li Xiao-Yong, Wang Guo-Li, Zhou Xiao-Xin

Chin. Phys. B . 2012, 21(9): 094205 . **doi:** 10.1088/1674-1056/21/9/094205

Photoelectron momentum distributions of single-photon ionization under a pair of elliptically polarized attosecond laser pulses*

Hui-Fang Cui(崔会芳)[1,2] and Xiang-Yang Miao(苗向阳)[1,2,†]

[1] College of Physics and Information Engineering, Shanxi Normal University, Linfen 041004, China
[2] Key Laboratory of Spectral Measurement and Analysis of Shanxi Province, Shanxi Normal University, Linfen 041004, China

(Received 18 February 2020; revised manuscript received 17 March 2020; accepted manuscript online 18 April 2020)

The attosecond ionization dynamics of atoms has attracted extensive attention in these days. However, the role of the initial state is not clearly understood. To address this question, we perform simulations on the neon atom and its model atom with different initial states by numerically solving the corresponding two-dimensional time-dependent Schrödinger equations. We theoretically investigate atomic photoelectron momentum distributions (PMDs) by a pair of elliptically polarized attosecond laser pulses. We find that the PMD is sensitive not only to the ellipticities of the pulses, the relative helicity, and time delay of the pulses, but also to the symmetry of the initial electronic states. Results are analyzed by the first-order time-dependent perturbation theory (TDPT) and offer a new tool for detecting the rotation direction of the ring currents.

Keywords: photoelectron momentum distributions, elliptically polarized attosecond laser pulses, magnetic quantum numbers, rotation direction of the ring currents

PACS: 42.50.Hz, 42.65.Re, 32.80.Wr **DOI:** 10.1088/1674-1056/ab8ac0

1. Introduction

With the development of high-order harmonic generation (HHG),[1–5] extreme ultraviolet (XUV) pulses are now routinely produced in table-top experiments, making it possible to directly observe the electron dynamics of atoms and molecules. The information about the atomic and molecular electronic wavefunction before ionization is imprinted on the momentum distribution of photoionized electrons. The first theoretical calculation on the ionization of arbitrarily spatially oriented H_2^+ was performed by using the attosecond laser field.[6] In 2013, Neidel *et al.*[7] firstly observed attosecond time-scale electron dynamics by using an attosecond pulse. In particular, the generation of circularly and/or elliptically polarized XUV pulses[8–10] opens up possibilities for studying and controlling effects and target properties that are not accessible with linearly polarized pulses. The circularly polarized attosecond laser pulses, especially the bichromatic circularly polarized attosecond laser pulses, are now being adopted to probe atomic and molecular structures by photoelectron momentum distributions.[11–17] For example, the investigations of ionization by two oppositely circularly polarized time-delayed XUV pulses have revealed helical vortex structures in atomic photoionization momentum distributions.[18–20]

According to the Bohr model, the electron moves around the nucleus on circular orbits possessing quantized orbital angular momentum associated with a ring current. In quantum mechanics, this motion is reflected by the magnetic quantum number m.[21] In the multiphoton ionization regime, most studies are based on the ground state (1s) as the initial state, the role of the magnetic quantum number was rarely taken into consideration. However, most of rare gas atoms, excited atoms and molecules can carry ring currents in microscopic media. In rare gas atoms, such as neon atom, the population of orbitals of positive m rotating anticlockwise and that of negative m rotating clockwise are equal, with resulting ring current being zero. The studies of ring currents can pave the way for detecting and controlling ultrafast processes on a nanoscale, including negative charge migration in many biological and chemical reactions[22–24] and chemical bond formation,[25] as well as for the generation of intense magnetic field pulses.[26,27]

In this paper, we numerically simulate the two-dimensional (2D) time-dependent Schrödinger equations for neon atom and its model atom under a pair of elliptically polarized attosecond laser pulses. We propose and theoretically explore a novel approach to characterizing the ultrafast ring current in media by a pair of oppositely elliptically polarized attosecond laser pulses. This scheme is implemented by using a pair of oppositely elliptically polarized attosecond laser pulses having the same carrier frequency, making it highly versatile. For the case of without time delay, the superposing of two attosecond laser pulses oppositely elliptically polarized with the same carrier-envelop phases (CEPs) gives a linearly polarized pulse. We observe the photoelectron momentum distribution (PMD) symmetric along the polarization

*Project supported by the National Natural Science Foundation of China (Grant Nos. 11404204 and 11974229), the Natural Science Foundation for Young Scientists of Shanxi Province, China (Grant No. 201901D211404), the Scientific and Technological Innovation Program of Higher Education Institutions in Shanxi Province, China (Grant No. 2019L0468), and the Project of Excellent Course of Shanxi Normal University, China (Grant No. 2017YZKC-35).

†Corresponding author. E-mail: sxxymiao@126.com

© 2020 Chinese Physical Society and IOP Publishing Ltd

axis (p_x axis) for the 1s orbital which is spherically symmetric. However, if the medium carries a ring current, under the same laser pulse, the PMD symmetry axis rotates an angle about the polarization axis, which is related to the direction of the ring current. In order to find out what other factors affecting the PMDs are, we also examine how the laser parameters, such as the ellipticity, the relative polarization, the relative CEPs and time delays, control the ejection angle of the maxima of the PMDs. Our results reveal that in the single-photon ionization of neon atom, the ejection angle is not only determined by the pulse parameters, but also described by the rotation direction of the initial current carrying orbitals. We also employ the first-order time-dependent perturbation theory (TDPT) to analyze the interaction between the XUV pulse and the atom. We find that the numerical results are consistent with those obtained by the perturbation theory.

2. Numerical methods and perturbation theory

2.1. Numerical methods

We numerically solve the two-dimensional time-dependent Schrödinger equation (TDSE) for neon atom and its model atom in rectangular plane coordinates $\boldsymbol{r} \equiv (x,y)$. The TDSE reads as (atomic units are used throughout this paper unless otherwise stated)

$$\mathrm{i}\frac{\partial \psi(\boldsymbol{r},t)}{\partial t} = H(\boldsymbol{r},t)\,\psi(\boldsymbol{r},t), \tag{1}$$

which is described by the Hamiltonian $H(\boldsymbol{r},t) = H_0(\boldsymbol{r},t) + H_{\rm int}(\boldsymbol{r},t)$ with the field-free term $H_0(\boldsymbol{r}) = T(\boldsymbol{r}) + V_{\rm C}(\boldsymbol{r})$, where the atomic kinetic operator is expressed as

$$T(\boldsymbol{r}) = -\frac{1}{2}\left(\frac{\partial^2}{\partial x^2} + \frac{\partial^2}{\partial y^2}\right) \tag{2}$$

and the soft-core Coulomb potential

$$V_{\rm C}(\boldsymbol{r}) = -\frac{Z(x,y)}{\sqrt{x^2+y^2+a}}. \tag{3}$$

We obtain the bound states of the field-free Hamiltonian H_0 by numerically solved the time-independent Schrödinger equation with the sine discrete-variable representation (sine-DVR).[28,29] For neon atom, the soft parameters $Z(x,y) = 1 + 9\exp(-x^2-y^2)$ and $a = 2.88172$ are used to remove the Coulomb singularity and to obtain the ionization potential $I_{\rm p} = 0.793$ a.u. (atomic unit) for the 2p orbitals. From the time-independent Schrödinger equation, we obtain two real 2p orbitals in the 2D Cartesian coordinate, that is, $2p_x$ and $2p_y$. The current-carrying orbital $2p_+$ ($2p_-$) with magnetic quantum number $m = +1$ ($m = -1$) is taken as the initial electron wave function $\psi(\boldsymbol{r},t=0)$, which is defined as $|\psi_{2p_\pm}\rangle = (|\psi_{2p_x}\rangle \pm \mathrm{i}|\psi_{2p_y}\rangle)/\sqrt{2}$. The quantum numbers $m = 1$ and $m = -1$ are projections of the angular momentum in the quantization axis (z axis, which is in the light propagation direction), which means that the electron ring currents in the (x, y) plane are counter-rotating and co-rotating with respect to the helicity of the laser pulse.[5] For reference calculations we use 1s as the initial state but keep the same ionization potential by taking $Z(x,y) = 1$ and $a = 0.1195$.[5] The term $H_{\rm int}(\boldsymbol{r},t)$ is the laser–electron interaction term, in the length gauge, which can be expressed as

$$H_{\rm int}(\boldsymbol{r},t) = xE_x(t) + yE_y(t), \tag{4}$$

where $E_x(t)$ and $E_y(t)$ are the x and y components of the laser electric field. The laser electric field is

$$\boldsymbol{E}(t) = \boldsymbol{E}_1(t) + \boldsymbol{E}_2(t) \tag{5}$$

with

$$\begin{aligned}\boldsymbol{E}_1(t) &= E_0 f(t)(\cos(\omega t+\phi_1)\boldsymbol{e}_x \\ &\quad + \varepsilon\sin(\omega t+\phi_1)\boldsymbol{e}_y)/\sqrt{1+\varepsilon^2}, \end{aligned}\tag{6}$$

$$\begin{aligned}\boldsymbol{E}_2(t) &= E_0 f(t-t_{\rm d})(\cos(\omega(t-t_{\rm d})+\phi_2)\boldsymbol{e}_x \\ &\quad \pm\varepsilon\sin(\omega(t-t_{\rm d})+\phi_2)\boldsymbol{e}_y)/\sqrt{1+\varepsilon^2}, \end{aligned}\tag{7}$$

where $t_{\rm d}$ represents the time delay between the two elliptically polarized attosecond laser pulses and ε is the ellipticity of the laser pulses. The sign "$\pm$" indicates that the two pulses are co-rotating ("+") or counter-rotating ("−") polarization. The laser pulse envelope $f(t) = \sin^2(\pi t/\tau)$ is used with a duration of $\tau = n_{\rm p}T$, where $T = 2\pi/\omega$ is the period of the laser field. E_0 is the maximum amplitude of the field, corresponding to a pulse intensity $I_0 = c\varepsilon_0 E_0^2/2$ which is fixed at 6×10^{13} W/cm^2.

The TDSE is propagated on a 2D Cartesian grid, obtained by using the parallel quantum wave-packet computer code LZH-DICP.[30,31] In our simulation, we set the length of the integration grid to be 480 a.u. A $\cos^{1/8}$ mask function is placed at x, $y = \pm200$ a.u. after each time evolution step in order to avoid the reflection of the wave function from the boundary. After the end of the laser pulse, the wave function further propagates for an additional ten optical cycles to ensure that all the ionized components move away from the core. Then we obtain the ionized wave function, $\psi_{\rm ion}(x,y) = M(r_{\rm b})\psi_{\rm final}(x,y)$, in the range of $x^2+y^2 > 50$ a.u., where $\psi_{\rm final}(x,y)$ is the wave packet at final time, $M(r_{\rm b})$ is an absorption function in the form of[32]

$$M(r_{\rm b}) = \frac{1}{1+\exp[-\beta(r-r_{\rm b})]}. \tag{8}$$

In the present simulation, we choose $\beta = 0.125$ a.u. and $r_{\rm b} = 50$ a.u. Finally, the final photoelectron momentum distribution (PMD) is obtained by applying Fourier transform to the ionized wave function as obtained below:

$$\begin{aligned}&\left|\tilde{\psi}(p_x,p_y)\right|^2 \\ &= \left|\frac{1}{2\pi}\iint \psi_{\rm ion}(x,y)\exp(-\mathrm{i}(xp_x+yp_y))\,\mathrm{d}x\mathrm{d}y\right|^2. \end{aligned}\tag{9}$$

2.2. Perturbation theory

In the present work, the simulations are conducted on the ionization process of neon atom and its model atom with elliptically polarized attosencond XUV pulses. The frequencies of the pulses are set to be $\omega = 1.0$ a.u. The Keldysh parameter $\gamma = \sqrt{I_p/2U_p} > 1$, where I_p is the ionization potential, implying that this is a multiphoton ionization process. Since $I_p = 0.793$ a.u., the single-photon ionization process is dominated. The first-order TDPT can be adopted to describe the ionization.[18,33] The first-order amplitude A_1 for the single-photon ionization of an atom by the electric field $\boldsymbol{E}(t)$ is defined as

$$A_1 = -\mathrm{i}\int_{t_0}^{t} \mathrm{d}t' \langle \psi_c | \boldsymbol{D}\cdot\boldsymbol{E} | \psi_0 \rangle \, \mathrm{e}^{\mathrm{i}\omega_{c0}t'}, \tag{10}$$

where $|\psi_0\rangle$ is the initial state with energy $-E_0$, $|\psi_c\rangle$ is the final continuum state of the electron with momentum $\boldsymbol{p} \equiv (p_x, p_y)$ and energy $E = p^2/2$, $\omega_{c0} = E + E_0$, and $\boldsymbol{D} = \boldsymbol{n}D$ is the dipole moment of the atom.

In this paper, the electric field $\boldsymbol{E}(t)$ in Eq. (5) can be written as

$$\begin{aligned}\boldsymbol{E}(t) \;=\; & E_0 f(t)\mathrm{Re}\left[\boldsymbol{e}_1 \exp\left(-\mathrm{i}(\omega t + \phi_1)\right)\right] \\ & + E_0 f(t-t_d)\mathrm{Re}\left[\boldsymbol{e}_2 \exp\left(-\mathrm{i}(\omega(t-t_d) + \phi_2)\right)\right], \end{aligned} \tag{11}$$

where $\boldsymbol{e}_j = (\boldsymbol{e}_x + \mathrm{i}\varepsilon_j \boldsymbol{e}_y)/\sqrt{1+\varepsilon_j^2}$ $(j = 1, 2)$ is the complex polarization vector normalized as $\boldsymbol{e}_j^* \cdot \boldsymbol{e}_j = 1$. Thus, the first-order TDPT amplitude in Eq. (10) for single-photon ionization of an atom under the pair of pulses takes the factorized form

$$A_1 = -\exp\left(-\mathrm{i}\phi_1\right)\alpha(p) A_\gamma, \tag{12}$$

where the parameter A_γ is in the form of

$$A_\gamma = \boldsymbol{n}\cdot(\boldsymbol{e}_1 + \boldsymbol{e}_2 \exp(\mathrm{i}\Phi)) \tag{13}$$

and the relative phase, Φ, is given by

$$\Phi = \omega t_d + (\phi_1 - \phi_2). \tag{14}$$

The relative phase Φ in Eq. (14) consists of two factors: ωt_d, the difference in the phase accumulation during the temporal evolution of the electronic wave packets for a time delay t_d, and the difference between the CEPs of the pair of pulses $(\phi_1 - \phi_2)$. The $\alpha(p) = |\alpha|\,\mathrm{e}^{\mathrm{i}\chi}$ depends on the ionizing laser pulse and the initial electronic state.

According to the first-order TDPT, for the two time-delayed elliptically identically polarized pulses in the polarization plane- (x, y) plane, *i.e.*,

$$\boldsymbol{e}_1 = \frac{(\boldsymbol{e}_x + \mathrm{i}\varepsilon\boldsymbol{e}_y)}{\sqrt{1+\varepsilon^2}}, \quad \boldsymbol{e}_2 = \boldsymbol{e}_1. \tag{15}$$

We define also the degree of linear and circular polarization of the pulse, l and ξ as shown in Ref. [18]:

$$l \equiv \frac{1-\varepsilon^2}{1+\varepsilon^2} = \boldsymbol{e}\cdot\boldsymbol{e}, \tag{16}$$

$$\xi \equiv \frac{2\varepsilon}{1+\varepsilon^2} = \mathrm{i}\boldsymbol{e}_z\cdot(\boldsymbol{e}\times\boldsymbol{e}^*). \tag{17}$$

Then

$$\boldsymbol{n}\cdot\boldsymbol{e}_1 = (\cos\varphi + \mathrm{i}\varepsilon\sin\varphi)/\sqrt{1+\varepsilon^2}, \tag{18}$$

where φ is the angle between $\boldsymbol{n}$ and the x axis and is also the ejection angle of the photoelectron defined in this work. The final PMD for ionization is

$$W_\varepsilon(\boldsymbol{p}) = |\alpha(p)|^2 [1 + l\cos(2\varphi)][1 + \cos(\Phi)], \tag{19}$$

where $|\alpha(p)|^2[1 + l\cos(2\varphi)]\cos(\Phi)$ is the interference term which is determined by the relative CEP, the time delay and the ellipticity of the laser pulses. For the two time-delayed elliptically oppositely polarized pulses, *i.e.*,

$$\boldsymbol{e}_1 = \frac{(\boldsymbol{e}_x + \mathrm{i}\varepsilon\boldsymbol{e}_y)}{\sqrt{1+\varepsilon^2}}, \quad \boldsymbol{e}_2 = \boldsymbol{e}_1^*, \tag{20}$$

$$\boldsymbol{n}\cdot\boldsymbol{e}_1 = (\cos\varphi + \mathrm{i}\varepsilon\sin\varphi)/\sqrt{1+\varepsilon^2}, \tag{21}$$

$$\boldsymbol{n}\cdot\boldsymbol{e}_2 = (\cos\varphi - \mathrm{i}\varepsilon\sin\varphi)/\sqrt{1+\varepsilon^2}. \tag{22}$$

The final PMD for ionization is

$$W_\varepsilon(\boldsymbol{p}) = |\alpha(p)|^2 [1 + l\cos(2\varphi)][1 + \cos(2\alpha - \Phi)], \tag{23}$$

where $\tan(\alpha) = \varepsilon\sin(\varphi)/\cos(\varphi)$, and

$$|\alpha(p)|^2[1 + l\cos(2\varphi)]\cos(2\alpha - \Phi)$$

is the interference term. According to previous research in Ref. [18], for the atom in its 1s ground state, the parameter $|\alpha(p)|^2$ depends only on the electron energy $E = p^2/2$ and is independent of the momentum direction. Therefore, the angular distribution for the 1s state is determined only by the parameter $|A_\gamma|^2$ which depends on pulse parameters $\boldsymbol{e}_1$, $\boldsymbol{e}_2$, t_d, and $(\phi_1 - \phi_2)$.

In this work, we present numerical results of neon atom and its model atom in different initial states for two laser cases: (i) the elliptically identically polarized pulses $\boldsymbol{e}_2 = \boldsymbol{e}_1$, *i.e.*, the co-rotating polarization case; (ii) the elliptically oppositely polarized pulses, $\boldsymbol{e}_2 = \boldsymbol{e}_1^*$, *i.e.*, the counter-rotating polarization case. We find that besides the laser pulse, the initial electronic state has also great influence on PMDs.

3. Numerical results and discussion

We first consider the single-photon ionization process of the model atom with the 1s state as the initial state. Figure 1 displays results of the single-photon ionization by a pair of elliptically polarized pulses at different values of ellipticity ε. According to the first-order perturbation theory, we show the relationship between the parameter $|A_\gamma|^2$ and the ejection angle φ in Figs. 1(i) and 1(j). For the case of co-rotating polarization, *i.e.*, $\boldsymbol{e}_1 = \boldsymbol{e}_2$, as l increases, the circular symmetry of the

PMD will be broken, the maxima appear at $\varphi = 0$ and $\varphi = \pi$, and the minima appear at $\varphi = \pi/2$ and $\varphi = 3\pi/2$. The magnitudes of the maxima decrease and those of minima increase as ε increases, which is presented in Fig. 1(i). For the case of counter-rotating polarization, *i.e.*, $\boldsymbol{e}_1 = \boldsymbol{e}_2^*$, from Fig. 1(j) we see that the positions of the maxima and the minima are same as those for the case $\boldsymbol{e}_1 = \boldsymbol{e}_2$, the magnitudes of maxima still decrease as ε increases, but those of minima do not change as ε increases and always stay 0. From Figs. 1(a)–1(h), one sees that the PMDs are sensitive to the ellipticities of the laser fields, as ε changes, the changes of magnitudes of the maxima and the minima are consistent with the TDPT results presented in Figs. 1(i) and 1(j).

We also study the effect of the pulse relative CEP $\phi_1 - \phi_2$ and the time delay t_d on the PMDs under a pair of identically polarized pulses at fixed ellipticity $\varepsilon = 0.25$, and the results are shown in Fig. 2. It can be seen from the figure that as predicted by Eq. (19), only the magnitudes of PMDs change with CEPs and time delay, while the distribution patterns remain unchanged.

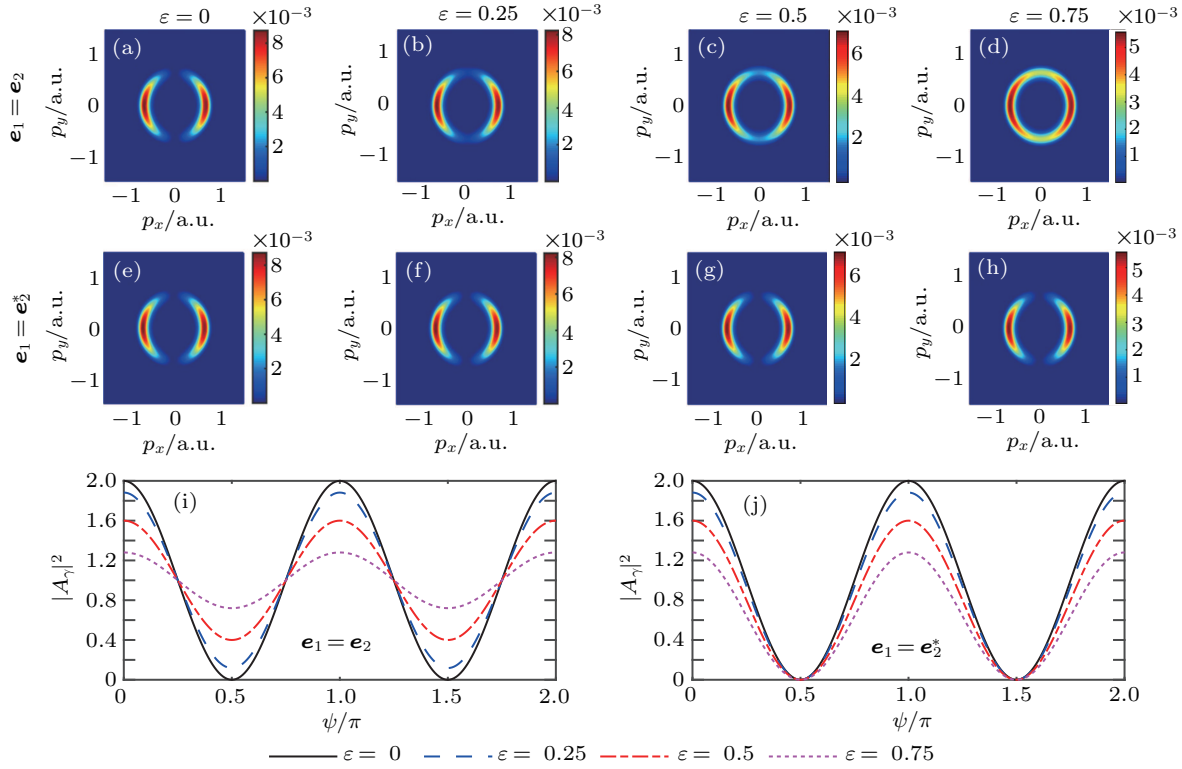


Fig. 1. Photoelectron momentum distributions of the model atom in panels (a)–(d) co-rotating polarization case and (e)–(h) counter-rotating polarization case at different ellipticities: (a) and (e) $\varepsilon = 0$, (b) and (f) $\varepsilon = 0.25$, (c) and (g) $\varepsilon = 0.5$, and (d) and (h) $\varepsilon = 0.75$. Panels (i) and (j) show theoretical results of the parameter $|A_\gamma|^2$ in co-rotating polarization case and counter-rotating polarization case, respectively.

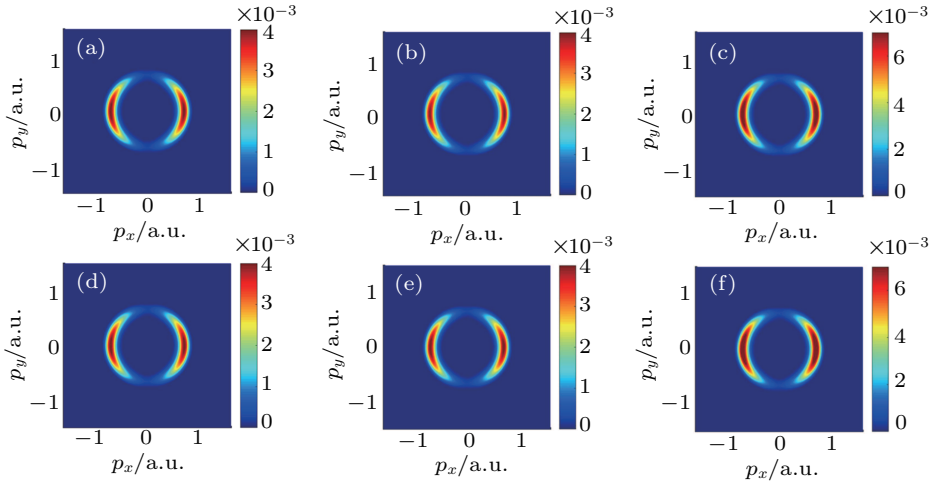


Fig. 2. Photoelectron momentum distributions of model atom in co-rotating polarization case at ellipticity $\varepsilon = 0.25$ with different time delays: (a) $\omega t_\mathrm{d} = 0.5\pi$, (b) $\omega t_\mathrm{d} = 1.5\pi$, (c) $\omega t_\mathrm{d} = 2\pi$; and with different CEPs: (d) $\phi_2 = 0.5\pi$, (e) $\phi_2 = 1.5\pi$, and (f) $\phi_2 = 2\pi$. Other laser parameters are the same as those in Fig. 1.

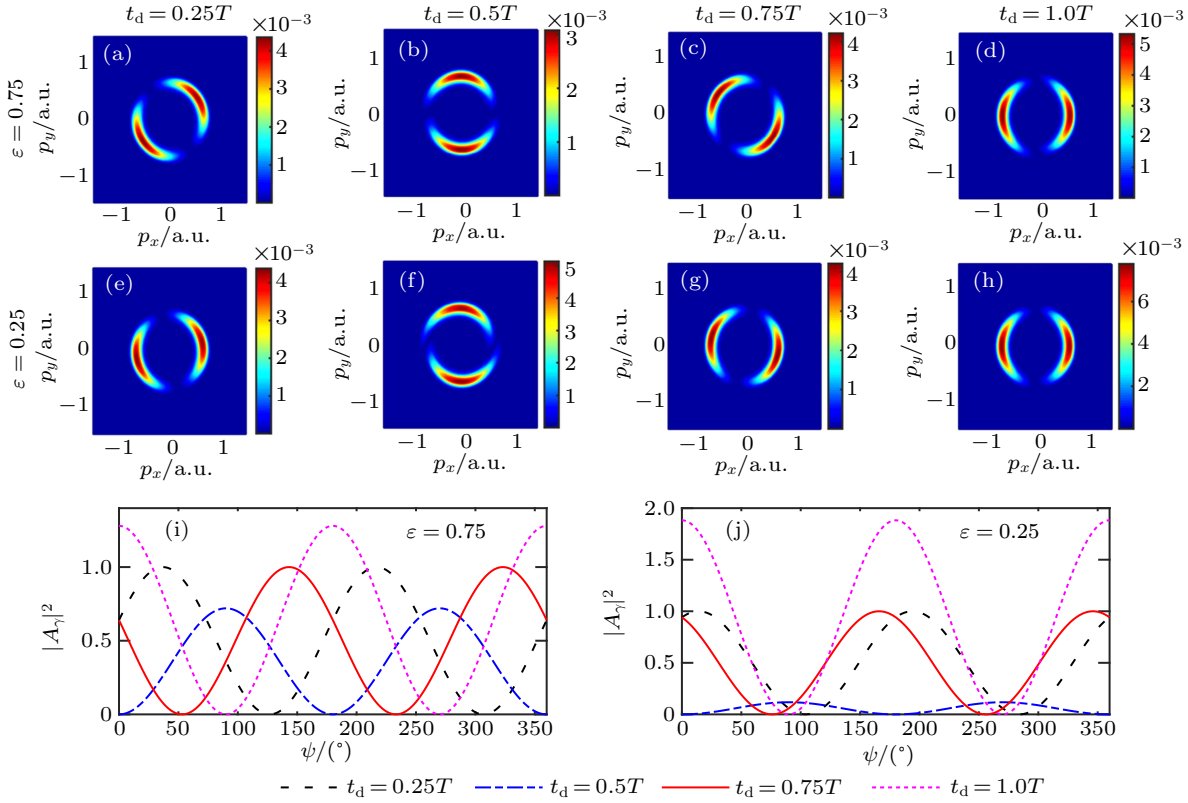


Fig. 3. Photoelectron momentum distributions of the model atom in counter-rotating polarization case at different ellipticities: [(a)–(d)] $\varepsilon = 0.75$ and [(e)–(h)] $\varepsilon = 0.25$ with time delays: (a) and (e) $\omega t_d = 0.5\pi$, (b) and (f) $\omega t_d = \pi$, $\omega t_d = 1.5\pi$, and (d) and (h) $\omega t_d = 2\pi$. (i) and (j) Theoretical results of parameter $|A_\gamma|^2$ at elliptivities: $\varepsilon = 0.75$ and $\varepsilon = 0.25$, respectively. Other laser parameters are the same as those in Fig. 1.

The numerical results of the model atom under a pair of time-delayed elliptically oppositely polarized pulses with different values of ellipticity ε are shown in Fig. 3. We also take the 1s state as an initial state. The other laser parameters are the same as those used for the identical case in Fig. 2. The PMDs at two pulse ellipticities, $\varepsilon = 0.75$ [Figs. 3(a)–3(d)] and $\varepsilon = 0.25$ [Figs. 3(e)–3(h)], four time delays, $t_d = 0.25T$ [Figs. 3(a) and 3(e)], $t_d = 0.5T$ [Figs. 3(b) and 3(f)], $t_d = 0.75T$ [Figs. 3(c) and 3(g)] and $t_d = 1.0T$ [Figs. 3(d) and 3(h)] are presented, respectively. As one can see from Fig. 3, for the elliptically oppositely polarized case, PMDs, especially the PADs, are sensitive to the pulse ellipticity ε and the time delay t_d. It is found that the time delay varying from $t_d = 0.25T$ to $t_d = 1.0T$ causes the PMDs to rotate counterclockwise different angles (different values of $\Delta\varphi$) under the laser pulses with different ellipticities. We next also use the first-order TDPT to describe the ejection angles of PMDs in Figs. 3(a)–3(h). From Eq. (23) one sees that $W_\varepsilon(\boldsymbol{p})$ is a function of ejection angle φ, relative pulse CEP $(\phi_1 - \phi_2)$, pulse ellipticity ε and time delay t_d. At fixed ellipticities $\varepsilon = 0.75$ and $\varepsilon = 0.25$, when the time delay changes, the corresponding $|A_\gamma|^2$ values are present in Figs. 3(i) and 3(j). As shown in Figs. 3(i) and 3(j), one sees that when the ellipticity is fixed, not only the magnitude, but also the ejection angle φ for each of the maxima and minima change with time delay. The corresponding angle shift $\Delta\varphi$ is a function of ε and t_d. The result is different from that for the case of two oppositely circularly polarized pulses at the same frequencies in Ref. [18]. The main reason for the difference is the dependence of the interference term on the ellipticity as indicated in Eq. (23).

Next, we study the effect of magnetic quantum number of the initial state on the patterns in PMDs by using a pair of time-delayed elliptically oppositely polarized pulses. We numerically simulate the photoionization process of neon atom of which the highest-occupied orbital is 2p orbital. The PMDs and the corresponding PADs of neon atom with different initial states under a pair of counter-rotating polarization laser pulses at different time delays with an ellipticity of 0.75 are displayed in Fig. 4. Comparing with the ejection angles of the maxima and minima of the model atom in Figs. 3(a)–3(d), there are angular shifts in the 2p cases. We also find that the different 2p states differ in angular shift from each other. The angular shift difference reflects the effect of the magnetic quantum number of the initial state on PMD. We also use the first-order TDPT to understand the angular shifts in Fig. 4. As shown in Eq. (10), the PMD is determined by the initial state. We notice that the electron probability density of the initial state $|\psi_{2p_+}\rangle(|\psi_{2p_-}\rangle)$ exhibits toroidal distribution and the electron rotates anticlockwise (clockwise). Based on the relationship

$$|\psi_{2p_\pm}\rangle = (|\psi_{2p_x}\rangle \pm \mathrm{i}|\psi_{2p_y}\rangle)/\sqrt{2} = |\psi_{2p_\pm}|\exp(\pm \mathrm{i}\eta), \quad (24)$$

where $\pm\eta$ is the argument of the complex wavefunction

$|\psi_{2p_\pm}\rangle$. One can obtain the first-order amplitude $A_\pm$ from Eq. (10) as follows:

$$A_\pm = -i\int_{t_0}^{t} dt'(\langle\psi_c|\boldsymbol{D}\cdot\boldsymbol{E}||\psi_{2p}|\exp(\pm i\eta)\rangle) \times \exp(i\omega_{c0}t'). \quad (25)$$

From Eq. (25), we can see that the transition matrix element $\langle\psi_c|\boldsymbol{D}\cdot\boldsymbol{E}||\psi_{2p}|\exp(\pm i\eta)\rangle$ is also a function of electronic state, which can encode the information about the sign of the magnetic quantum number. However, the argument of the complex wavefunction, $\pm\eta$, cannot be added directly to the cos term such as $\cos(2\alpha-\Phi\pm\eta)$ because η is a function of (x, y). We surmise that the angular shift is related to the sign of the 2p state and the simulation results confirm our suspicions. We rewrite Eq. (23) as follows:

$$W_\varepsilon^\pm(\boldsymbol{p}) \propto [1+\cos(2\alpha-\Phi\pm\theta)], \quad (26)$$

where θ is the deflection angle compared with the result from Eq. (23) in the 1s case. From Figs. 4(b) and 4(d), we note that without the time delay, the maxima of the photoelectron angular distribution appear at around 60° and -120° for the $2p_+$ state, while the maxima appear at around -60° and 120° for the $2p_-$ state. This conclusion is consistent with our conjecture. We also find that the direction of angular shift is the same as the rotation direction of ring current in the case of 2p orbital.

In order to explore the relation between the angular shifts and the time delay for neon atom, we present the PMDs and corresponding photoelectron angular distributions (PADs) of the $2p_+$ and $2p_-$ at two different time delays $t_d = 0.25T$ [Figs. 4(e)–4(h)] and $t_d = 0.75T$ [Figs. 4(i)–4(l)]. For the time delay of $t_d = 0.25T$, we obtain the PADs shown in Figs. 4(f) and 4(h) for the $2p_+$ and $2p_-$ orbitals, respectively. The result in Fig. 4(f) shows that for the $2p_+$ case, the maxima appear at around 100° and 280°. Compared with the case without time delay, the corresponding angle shift $\Delta\varphi \approx 40^\circ$. For the 2p case, as shown in Fig. 4(h), the maxima appear at around -20° and 160°, of which the corresponding angle shift is also $\Delta\varphi \approx 40^\circ$ compared to the case without time delay. When time delay $t_d = 0.75T$, for both of the 2p orbitals, the corresponding angle shifts $\Delta\varphi \approx 140^\circ$, which is compared with the case without time delay [as shown in Figs. 4(j) and 4(l)]. From the above results it can be found that the varying of the time delay causes the PMDs to rotate counterclockwise an angular shift $\Delta\varphi$, of which the value is the same as that of 1s orbital under the same conditions.

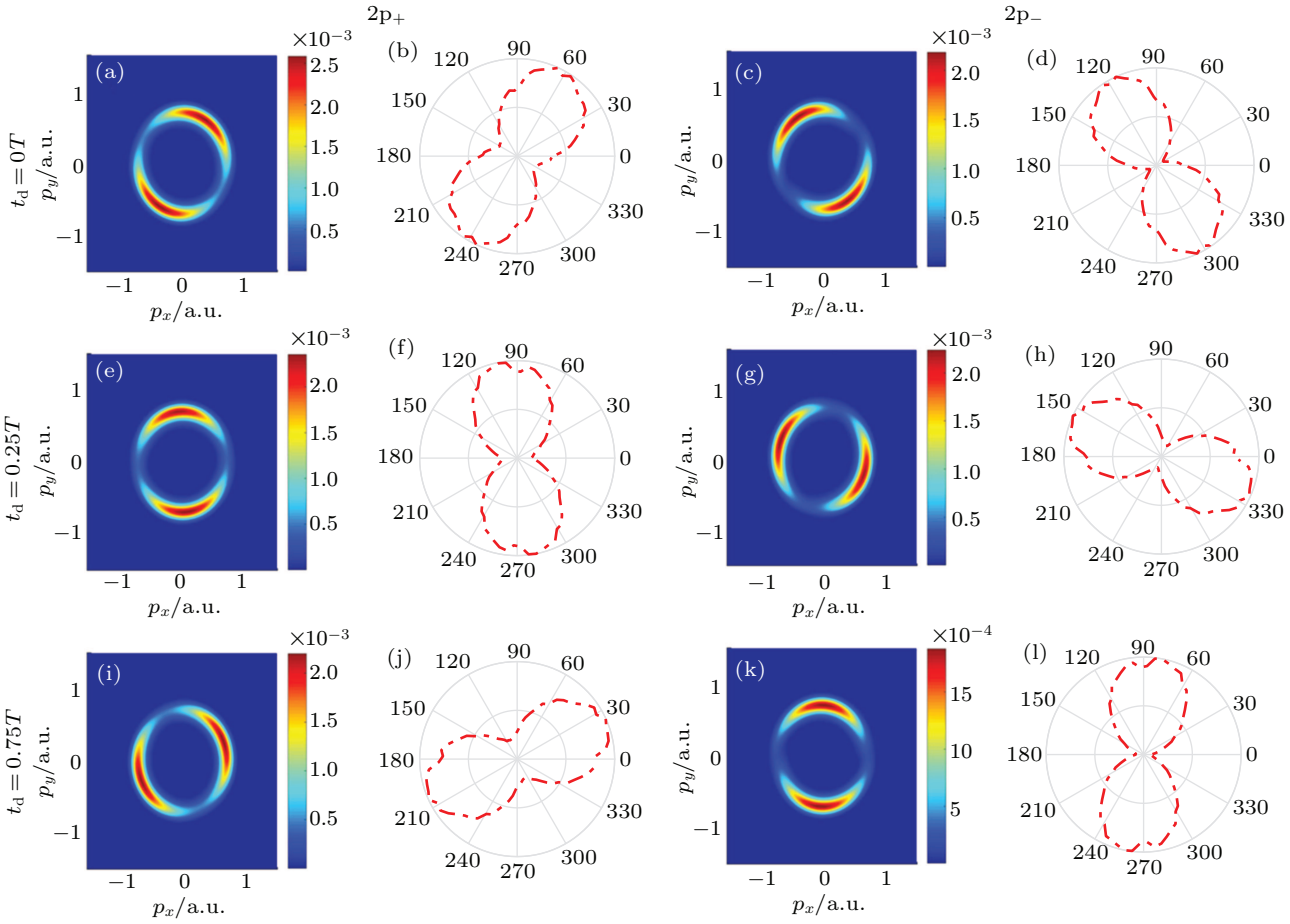


Fig. 4. Photoelectron momentum distributions and photoelectron angular distributions of neon atom in counter-rotating polarization case with initial states: [(a)–(d)] $2p_+$ and [(e)–(h)] 2p at time delays: [(a)–(d)] $\omega t_d = 0$ [(e)–(h)], $\omega t_d = 0.5\pi$, and [(i)–(l)] $\omega t_d = 1.5\pi$. Laser ellipticity is $\varepsilon = 0.75$ and other laser parameters are the same as those in Fig. 1.

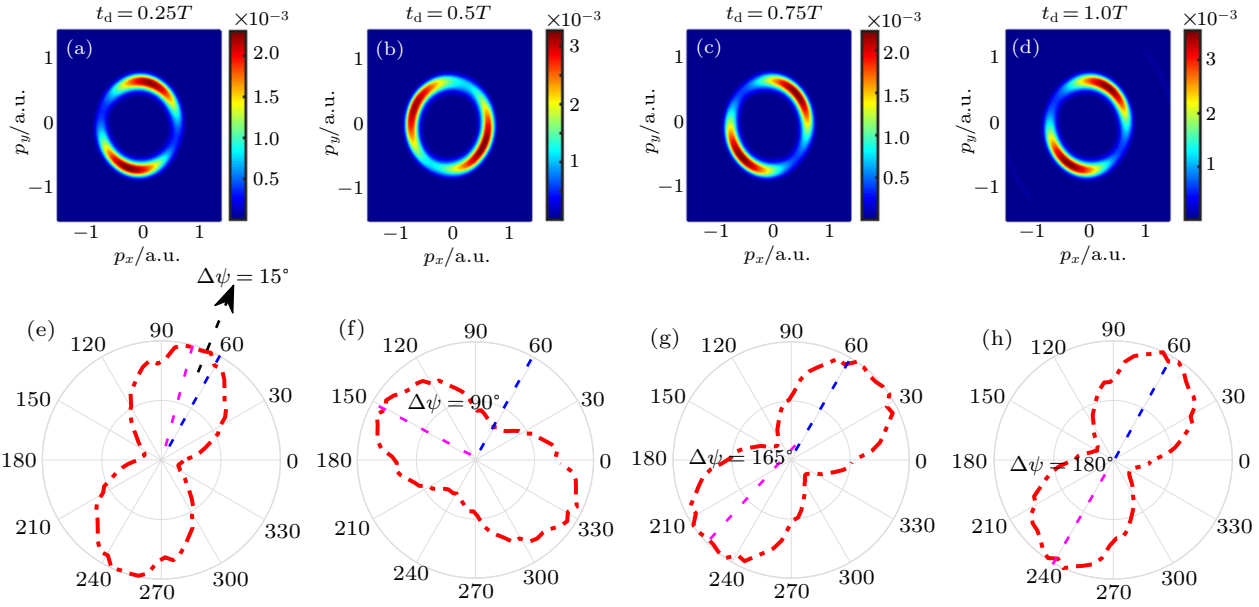


Fig. 5. [(a)–(d)] Photoelectron momentum distributions and [(e)–(h)] photoelectron angular distributions of neon atom under a pair of counter-rotating polarization laser pulses with initial state $2p_+$ at time delays: (a) and (e) $\omega t_d = 0.5\pi$, (b) and (f) $\omega t_d = \pi$, (c) and (g) $\omega t_d = 1.5\pi$, and (d) and (h) $\omega t_d = 2\pi$. Laser ellipticity is $\varepsilon = 0.25$ and other laser parameters are the same as those in Fig. 1.

To verify our conclusion, we display the PMDs and the corresponding PADs of photoionization for neon atom with the $2p_+$ initial state under a pair of time-delayed elliptically oppositely polarized pulses with an ellipticity of 0.25 in Fig. 5. One can see that the angular shifts [shown in Figs. 5(e)–5(h)] are also in good agreement with the predictions in Eq. (23) [as shown in Fig. 3(j)]. We also compare the magnitudes of PMDs in Fig. 4 with those in Fig. 5. It is found that the magnitudes of PMDs change with time delay and ellipticity for the $2p_+$ orbital in the same way as those for the 1s orbital in Fig. 3.

In addition, we carry out a lot of other calculations and find that for the same 2p orbital in the same laser frequency conditions, the deflection angle θ is the same, that is, θ is a constant. For example, the PMDs of $2p_+$ orbital under a pair of co-rotating polarization pulses are also calculated, the results show that the changing of the time delay will only result in the change of PMD magnitude and the ejection angles of the maxima are always stay at 60° and -120°. Therefore, under a pair of time-delayed laser pulses, the rotation direction of photoionization yield only depends on time delay and but not on the sign of the initial 2p state, which is consistent with the result in Eq. (26).

4. Conclusions and perspectives

Atomic photoionization of neon atom and its model atom under a pair of elliptically polarized attosecond laser pulses having the same frequencies are studied by numerically solving the 2D time-dependent Schrödinger equations. Two photoionization schemes of photoionization by a pair of elliptically polarized attosecond laser pulses with the same or opposite helicities are taken into account. Under the action of such high frequency attosecond laser pulses, the electron directly reaches from the bound state to the continuum state after it has absorbed a photon without initiating any additional dynamic behavior in ionization process. Photoelectrons with the same kinetic energy can be produced in the continuum after absorbing one photon in each pulse, thus triggering the ionization interference effect of the continuum electron wave functions. The interference between the wave functions causes the PMDs to be strongly dependent on relative pulse helicity, relative CEPs and time delay. In particularly, when the time delay between the two oppositely elliptically polarized attosecond laser pulses is changed, the ejection angles corresponding to the maxima and minima of the distributions are shifted, which gives rise to a rotation of PMDs. We adopt the first-order TDPT to describe the dependence of the interference patterns on laser parameters.

In addition, we find that the PMD is also determined by the magnetic quantum number of the initial state. The most important is that the maxima and minima of PMDs corresponding to the $2p_+$ state and $2p_-$ state have significant angular shift from the 1s state. The value of the angular offset reflects the rotation direction of the ionized orbital.

In summary, the patterns in PMDs are shown to be sensitive to the parameters of laser pulses and the magnetic quantum number of the initial state, which allows us to characterize the pulses and monitor the rotation direction of the ionized orbitals in the ultrafast photoionization process.

Acknowledgment

The authors sincerely thank Prof. Keli Han and Prof. Ruifeng Lu for providing us with the LZH-DICP code.

References

[1] Krause J L, Schafer K J and Kulander K C 1992 *Phys. Rev. Lett.* **68** 3535

[2] Popmintchev T, Chen M C, Arpin P, Murnane M M and Kapteyn H C 2010 *Nat. Photon.* **4** 822

[3] Milosevic D B 2015 *Phys. Rev. A* **92** 043827

[4] Baykusheva D, Ahsan M S, Lin N and Wörner H J 2016 *Phys. Rev. Lett.* **116** 123001

[5] Medišauskas L, Wragg J, van der Hart H and Ivanov M Y 2015 *Phys. Rev. Lett.* **115** 153001

[6] Selstø S, Førre M, Hansen J P and Madsen L B 2005 *Phys. Rev. Lett.* **95** 093002

[7] Neidel C, Klei J, Yang C H, Rouzée A, Vrakking M J J, Klünder K, Miranda M, Arnold C L, Fordell T, L'Huillier A, Gisselbrecht M, Johnsson P, Dinh M P, Suraud E, Reinhard P G, Despré V, Marques M A L and Lépine F 2013 *Phys. Rev. Lett.* **111** 033001

[8] Chen Z Y and Pukhov A 2016 *Nat. Commun.* **7** 12515

[9] Ma G, Yu W, Yu M Y, Shen B and Veisz L 2016 *Opt. Express* **24** 10057

[10] Huang P C, Hernández-García C, Huang J T, Huang P Y, Lu C H, Rego L, Hickstein D D, Ellis J L, Jaron-Becker A, Becker A, Yang S D, Durfee C G, Plaja L, Kapteyn H C, Murnane M M, Kung A H and Chen M C 2018 *Nat. Photon.* **12** 349

[11] Zhang H D, Ben S, Xu T T, Song K L, Tian Y R, Xu Q Y, Zhang S Q, Guo J and Liu X S 2018 *Phys. Rev. A* **98** 013422

[12] Yuan K J, Chelkowski S and Bandrauk A D 2015 *J. Chem. Phys.* **142** 144304

[13] Yuan K J, Chelkowski S and Bandrauk A D 2016 *Phys. Rev. A* **93** 053425

[14] Yuan K J and Bandrauk A D 2017 *Phys. Chem. Chem. Phys.* **19** 25846

[15] Yuan K J, Shu C C, Dong D Y and Bandrauk A D 2017 *J. Phys. Chem. Lett.* **8** 2229

[16] Yuan K J and Bandrauk A D 2019 *J. Phys. Chem. A* **123** 1328

[17] Wu W Y and He F 2016 *Phys. Rev. A* **93** 023415

[18] Ngoko Djiokap J M, Hu S X, Madsen L B, Manakov N L, Meremianin A V and Starace A F 2015 *Phys. Rev. Lett.* **115** 113004

[19] Ngoko Djiokap J M, Meremianin A V, Manakov N L, Hu S X, Madsen L B and Starace A F 2017 *Phys. Rev. A* **96** 013405

[20] Li M, Zhang G Z, Kong X L, Wang T Q, Ding X and Yao J Q 2018 *Opt. Express* **26** 878

[21] Barth I and Smirnova O 2011 *Phys. Rev. A* **84** 063415

[22] Hermann G, Liu C, Manz J, Paulus B, Pérez-Torres J F, Pohl V and Tremblay J C 2016 *J. Phys. Chem. A* **120** 5360

[23] Jia D, Manz J, Paulus B, Pohl V, Tremblay J C and Yang Y 2017 *Chem. Phys.* **482** 146

[24] Yuan K J and Bandrauk A D 2016 *J. Chem. Phys.* **145** 194304

[25] Rechtsman M C, Zeuner J M, Plotnik Y, Lumer Y, Podolsky D, Dreisow F, Nolte S, Segev M and Szameit A 2013 *Nature* **496** 196

[26] Yuan K J and Bandrauk A D 2015 *Phys. Rev. A* **92** 063401

[27] Zhang X F, Zhu X S, Wang D, Li L, Liu X, Liao Q, Lan P F and Lu P X 2019 *Phys. Rev. A* **99** 013414

[28] Muckerman J T 1990 *Chem. Phys. Lett.* **173** 200

[29] Colbert D T and Miller W H 1992 *J. Chem. Phys.* **96** 1982

[30] Cao X, Jiang S C, Yu C, Wang Y H, Bai L H and Lu R F 2014 *Opt. Express* **22** 26153

[31] Lu R F, Zhang P Y and Han K L 2008 *Phys. Rev. E* **77** 066701

[32] Jia J C, Cui H F, Zhang C P, Shao J, Ma J L and Miao X Y 2019 *Chem. Phys. Lett.* **725** 119

[33] Pronin E A, Starace A F, Frolov M V and Manakov N L 2009 *Phys. Rev. A* **80** 063403